Available online at www.sciencedirect.com

ScienceDirect

Procedia CIRP 58 (2017) 434 – 439

www.elsevier.com/locate/procedia

16th CIRP Conference on Modelling of Machining Operations

SWARM optimization of force model parameters in micromilling

Attanasio A.[a*], Ceretti E.[a], Giardini C.[b]

[a]*University of Brescia, Via Branze 38, 25123 Brescia, Italy*
[b] *University of Bergamo, Via Marconi 5, 24044 Dalmine, Italy*

* Corresponding author. Tel.: +39-030-371-5584; fax: +39-030-370-2448. *E-mail address:* aldo.attanasio@unibs.it

Abstract

Because of the improvement of machine-tool and tool performances in micro cutting field, the interest on these processes is increasing. Therefore, researchers involved in micro manufacturing processes focused their attention on these types of processes with the aim of improving the knowledge on the phenomena occurring during micro cutting operations.
The objective of this work is to develop a modelling procedure for forecasting cutting forces in micromilling considering the tool run-out and the cutting tool geometry. The designed modelling procedure combines information coming from a force model, an optimization strategy and some experimental tests. The implemented force model is based on specific cutting pressure and actual instantaneous chip section. The tool run-out and the cutting tool geometry were considered in the analytical model. The adopted optimization strategy was based on the Particles Swarm strategy due to its suitability in solving analytical non-linear models. The experimental tests consisted in realizing micro slots on a sample made of Ti6Al4V. The comparison between experimental and analytical data demonstrates the good ability of the proposed procedure in correctly defining the model parameters.

Peer-review under responsibility of the scientific committee of The 16th CIRP Conference on Modelling of Machining Operations

Keywords: micro milling, analitical model, optimization, SWARM, Titanium alloy

1. Introduction

Advanced technological fields, such as biomedical, medical, electronic, military, automotive and aerospace, play a fundamental role in the development of part miniaturization. The need of having small and precise parts is essential for industries involved in these fields. Manufacturing micro components (i.e., at least one dimension of the part is of the order of millimeter) allows:

- to miniaturize the devices used in biomedical laboratories (Lab-on-chips, …)
- to reduce the heat generated by the electronical devices
- to decrease the components weight reducing the fuel consumption

For this reason, several international research centers are studying the phenomena involved in the micro manufacturing processes.

Micro features can be obtained through different manufacturing processes based on conventional or non-conventional methods of material removal. Amongst them micro cutting processes show to be the most flexible allowing to realize 3D complex geometries. It is well known that micro cutting operations cannot be considered a downsizing of meso/macro cutting operations since physical phenomena neglected in meso/macro scale affect the material removal mechanism. During cutting, two different material removal mechanisms can take place, namely ploughing or shearing regime. Ploughing regime is an undesired condition since the material is not removed but ploughed. To avoid this regime it is necessary to set the process parameters (feed rate and depth of cut) in order to have an uncut chip thickness higher than the minimum chip thickness value. In this manner, the removal process is dominated by a shearing regime. The value of the minimum chip thickness depends on tool material and geometry [2] and on workpiece material [3].

Peer-review under responsibility of the scientific committee of The 16th CIRP Conference on Modelling of Machining Operations
doi:10.1016/j.procir.2017.03.248

Another parameter strongly affected by the dimensional scale is the Specific Shear Energy (SSE) [2]. This parameter corresponds to the energy needed for realizing the material removal. Finally, when approaching micromilling processes it is essential to know how process parameters, tool geometry and the tool-machine pairs affect the general cutting process and the final part quality in terms of surface roughness and accuracy [4].

The aim of this work is to develop a procedure for modeling the cutting forces generated during micromilling of slots. Some aspects have to be considered when approaching cutting force analysis in micro scale.

First of all the cutting forces measurement needs dynamometer characterized by high sensitivity and bandwidth because of the high spindle rotation regime of the order of thousand round per minute [5]. The acquired signal has to be fixed in order to reduce the signal noise [6]. Then, when modeling cutting forces in micromilling, tool run-out can not be neglected since it plays an important role. In fact, being the run-out value of the same order of magnitude of the feed per tooth, it affects the chip section and as a consequence the cutting force. FEM and Analytical models for micro-end milling operations including tool run-out are described in [7-11], while in [12] a new approach for evaluating micro-milling cutting forces, considering ploughing regime and tool run-out effect, is reported.

In this paper the developed procedure, its calibration and testing are described. The analytical force model was developed taking into account the tool run-out contribution and its influence on chip thickness in order to develop a consistent analytical model able to predict forces in micromilling. The developed analytical model was calibrated and tested using data coming from experimental tests made on Ti6Al4V alloy. This alloy was chosen since it is widely used in several advanced fields such as energy, medicine, biotechnology and automotive. In particular, a lamellar microstructure was obtained through customized heat treatment [13, 14]. All the model parameters were optimized by using Particles Swarm Optimization [15], an algorithm suitable for optimizing non linear problems.

2. Model optimization

2.1. Introduction

Fig. 1 reports a schematization of the activities involved in the optimization of an analytical model. Three inputs must be carefully defined before running the optimization algorithm:

1. the analytical model of the investigated phenomenon: in this work a model of cutting force in micromilling;
2. the experimental data: from an experimental campaign realized with the aim of measuring cutting forces;
3. the objective function: it is an analytical function representing the objective.

Then, the optimization algorithm (Particle Swarm Optimization algorithm in this work) iterates searching the best model parameters set that minimizes (or maximizes) the objective function according to the collected data.

2.2. Experimental test

A five axis ultra precision CNC machining center (KERN Pyramid Nano) was utilized for the experimental campaign. A sample made of Ti6Al4V alloy and heat treated in order to obtain a fully lamellar (or Widmanstätten) microstructure (Fig. 2a) was machined realizing three microchannels under the same cutting conditions. Each channel, characterized by a rectangular section 10 μm depth and a width equal to the tool diameter, was realized using a new tool. In this manner the influence of the tool wear on cutting forces was avoided.

Two flutes tungsten carbide micro end mills 200 μm diameter made by Mitsubishi (specification MS2SS D0020) were used. The cutting edge radius, measured by means of a Scanning Electron Microscope with a resolution of 10 nanometers, was equal to 5 μm.

All tests were realized under the same cutting conditions, selecting the following cutting parameters according to the data sheet of the tool:

- feed per tooth: 13 μm - higher than the cutting edge radius (5 μm) in order to guarantee a shear regime after the initial phase of cutting where ploughing regime is present;
- axial depth of cut (ap): 10 μm – it corresponds to the channel depth;
- cutting speed: 28 m/min (45000 rpm);
- lubrication: dry.

During cutting operations the cutting force components are acquired using piezoelectric force sensor (Type 9317C) made by Kistler, characterized by a natural frequency of 5 kHz. The force sensor has been carefully aligned to the machine tool axis (XYZ) in order to correctly acquire the force components along these directions. Kistler charge amplifiers (Type 5015A) intensifies the charge signals coming from the piezoelectric load cell and converts them into a proportional voltage output signals. These signals are acquired by a National Instrument cDAQ-9174 equipped with National Instruments 9205 board, and managed by a Virtual Instrument developed under Labview environment. Sampling frequency is set on 25 kHz in order to obtain a good signal resolution and to avoid aliasing effect.

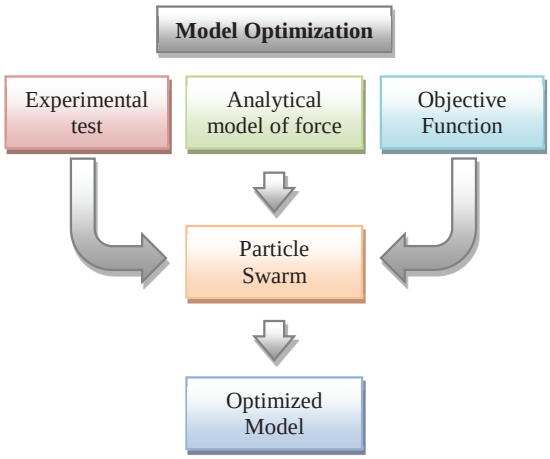

Fig. 1. Optimization chart.

Fig. 2b shows the cutting forces measured in a round during three different tests. It is possible to distinguish the cutting force distribution on each teeth of the mill (i.e., two maxima).

Tool run-out leads to different loads on mill teeth. This unbalanced load causes an increase of the difference of maximum peaks height and a different cutting time of each tooth (width of the bulges). For this reason, a different height of peaks is noticeable for test B and test C. Concerning test A, due to the bulges similarity it is possible to state that the tool run-out is very low. During the experiments no mill chatter was observed.

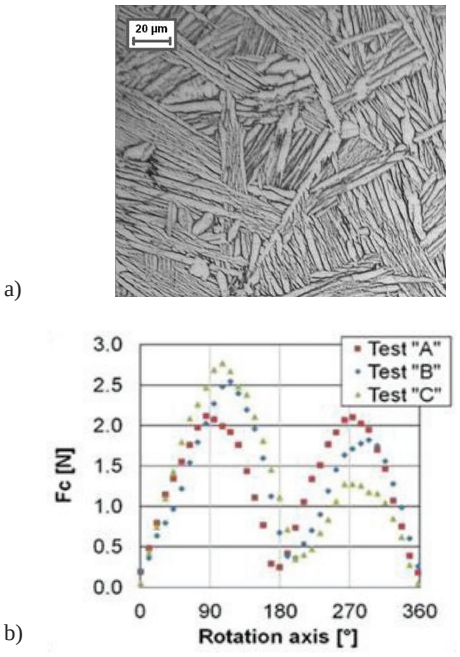

Fig. 2. (a) Sample microstructure (Ti6Al4V); (b) forces measured during the tests.

2.3. Analytical model of force

Tool run-out is due to a non-perfect alignment of spindle, tool-holder and tool axes. This misalignment generates cutting edges trajectories different from the theoretical trajectories. Therefore, the feed per tooth of the single tool tooth increases or decreases giving different values of instantaneous chip thickness and cutting force, as shown in Fig. 2b. Fig.3a reports the geometrical schematization of the cutting edges (namely CE1 and CE2) trajectories of a 2 flutes end-mill considering the tool run-out effect. Equations describing trajectories and actual chip thickness of each cutting edge are completely described in [16].

The Kronenberg formulation was used for developing the analytical model of forces. The material elastic springback was neglected since its influence is predominant in ploughing regime. This cutting condition was not considered in the present research, since in industrial practice it is an undesirable condition. The mill deflection due to the low micro tool stiffness was neglected too being low the measured cutting force (see Fig. 2b).

According to Eq. 1 and Eq. 2, the instantaneous chip section (S) of each cutting edge can be estimated as product between instantaneous chip thickness (h_{CE1} or h_{CE2} as defined in [16]) and depth of cut (DOC).

$$S_{CE1} = h_{CE1} \cdot DOC \qquad for\ 0 \le \omega t < \alpha \tag{1}$$

$$S_{CE2} = h_{CE2} \cdot DOC \qquad for\ \alpha \le \omega t < 2\pi \tag{2}$$

Where:

- DOC=ap=10 µm
- t=time [s]
- ω=spindle speed [rad/s]
- α=phase between mill teeth

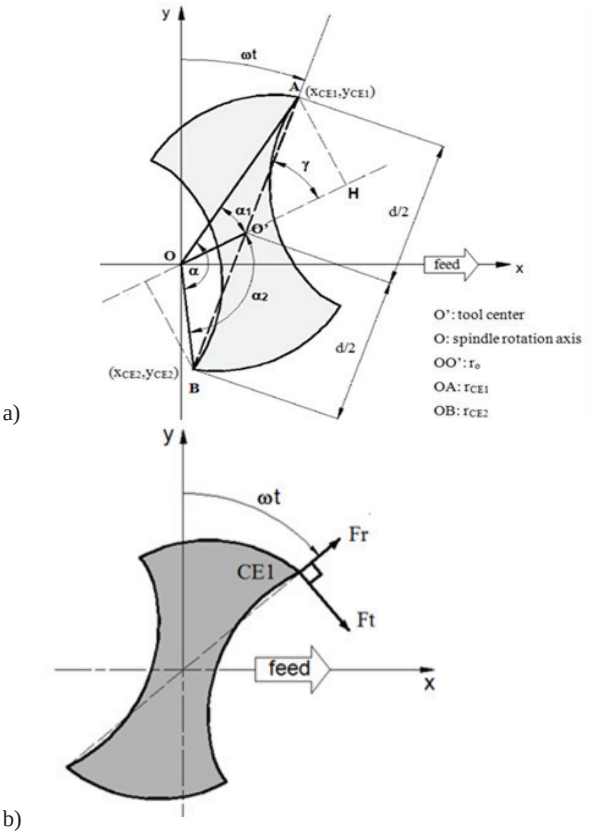

Fig. 3. Schematization of: (a) cutting edges trajectories with tool run-out; (b) tangential and radial forces during milling operations.

According to the Kronenberg theory, tangential component of the cutting force (Fig. 3b) was calculated as product between the cutting pressure (K_S) and the instantaneous chip section (S), (Eq. 3).

$$F_t = K_S \cdot S \tag{3}$$

Since the cutting pressure is function of the instantaneous chip section (S), K_S can be estimated by Eq. 4.

$$K_S = K_{S0} \cdot S^{-\frac{1}{m}} \quad (4)$$

K_{S0} (namely specific cutting pressure) and m are function of the tool-workpiece pair and they have to be experimentally estimated.

The radial force component can be obtained from the tangential force through a proportional factor (p) depending on friction conditions (Eq. 5).

$$F_r = F_t \cdot p \quad (5)$$

The cutting force components along x (or feed) and y (or cross feed) directions can be derived from tangential and radial components by (Eq. 6) and (Eq. 7).

$$F_{x\_model} = F_t \cdot cos\omega t + F_r \cdot sin\omega t \quad (6)$$

$$F_{y\_model} = F_t \cdot sin\omega t + F_r \cdot cos\omega t \quad (7)$$

2.4. Objective function

The objective function implemented in the optimization algorithm is reported in Eq. 8. Two terms can be identified: the first estimates the error of the x force component (F_{x_model}); the second refers to the error of the y force component (F_{y_model}). In this manner the optimization algorithm can give a set of model parameters that is the best compromise between x and y force components.

$$Err = \sum_{i=1}^{N} \left[\begin{matrix} \left(F_{x,model,i} - F_{x,exp,i}\right)^2 \cdot F_{x,exp,i} + \\ \left(F_{y,model,i} - F_{y,exp,i}\right)^2 \cdot F_{y,exp,i} \end{matrix} \right] \quad (8)$$

2.5. Swarm optimization

Table 1 summarizes the force analytical model parameters to optimize. It is possible to subdivide these parameters in two sets:

1. material parameters: refer to the material constants (K_{S0} and m) and the proportional factor (p);
2. tool run-out parameters: (r_o and γ), refer to the tool run-out contribute (see Fig. 3a).

The optimization algorithm to use must be selected taking into account that:

- the algorithm has to be suitable for the considered phenomenon;
- the algorithm has to be able to provide good and accurate results;
- the computational time has to be short.

Considering these characteristics, the Particle Swarm Optimization (PSO) algorithm [15] was selected. This optimization algorithm can be successfully used for minimizing and solving non-linear problems as the considered one.

Table 1. Model parameters.

Material	Run-out
Kronenberg experimental exponent (m)	Length (r_o)
Specific Cutting Pressure (K_{S0})	Angle (γ)
Proportional Factor (p)	

PSO algorithm is based on particles (candidates solutions) of a population (namely Swarm) which search for the maximum or the minimum of a defined objective function (measure of quality) moving in the n-dimensional hyperspace where the problem is defined. Each particle searches the problem solution according to mathematical formulae over its velocity ($v_{i,d}$ in Eq. 9) and its position ($x_{i,d}$ in Eq. 10). The research of the global best solution is realized considering the previous position ($p_{i,d}(t)$, particle or local best known position) and interaction of each particle with all the others particles ($g_{i,d}(t)$, hyperspace or swarm best known position).

$$\begin{aligned} v_{i,d}(t+1) = \omega \cdot v_{i,d}(t) + r_p \cdot \varphi_p \cdot \left(p_{i,d}(t) - x_{i,d}(t)\right) \\ + r_g \cdot \varphi_g \cdot \left(g_{i,d}(t) - x_{i,d}(t)\right) \end{aligned} \quad (9)$$

$$x_{i,d}(t+1) = x_{i,d}(t) + v_{i,d}(t+1) \quad (10)$$

Where r_p and r_g are two random numbers; ω is the global weight; φ_p and φ_g are respectively the particle factor and swarm factor.

The choice of PSO parameters (ω, φ_p, φ_g), of swarm size (i.e., number of particles *i*), and of maximum number of iterations is fundamental for the performance of the optimization algorithm. For this reason, a tuning of the PSO parameters was done with the aim of correctly balancing the exploration and deepening abilities of the algorithm in order to prevent a non-convergence of the iterations or a premature convergence to a local optimum point. Table 2 summarizes for each PSO parameter the investigated ranges and the corresponding steps used during the tuning phase.

All the analyses were performed using a freeware toolbox (PSO toolbox) implemented in Matlab® environment.

After the tuning phase, realized using the experimental data coming from test A, a maximum number of 2000 iterations and 200 particles were set; global weight, particle factor and swarm factor were set respectively equal to 0.0004, 1.2 and 0,012. These values were choose since they give the minimum error for the selected objective function (Eq. 8). Figure 4 shows the good agreement between the experimental force and the model forces at the end of the tuning phase.

Table 2. PSO parameters (ω, φ_p, φ_g), swarm size and maximum iteration tested during the tuning phase: range and step.

	Range	Step size
Global weight (ω)	0 ÷ 4	0.5
Particle factor (φ_p)	0 ÷ 4	0.5
Swarm factor (φ_g)	0 ÷ 1	0.1
Swarm size (i)	50 ÷ 200	50
Maximum number of iterations	500 ÷ 2000	500

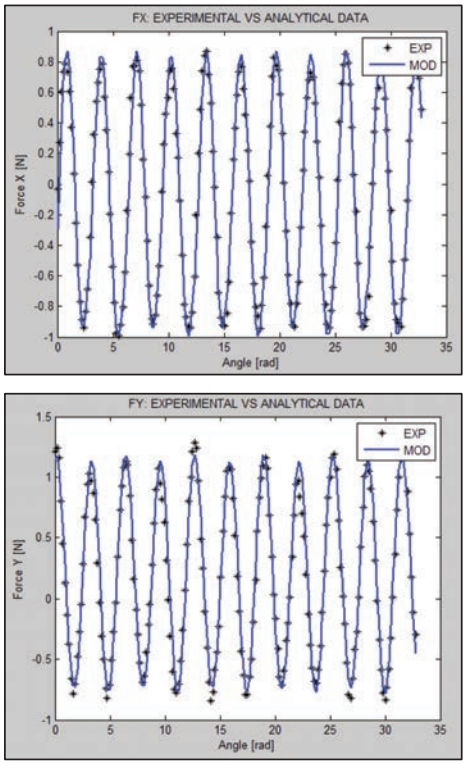

Fig. 4. Experimental force vs. model force (X and Y components).

3. Results discussion

Table 3 reports for each test the best set of model parameters.

Concerning the material parameters (K_{S0}, m, and p), they were defined using the data coming from test A, since low run-out was noticed during this test (see Figure 2b). Then, Test B and Test C were optimized keeping constant the values of these parameters. The model uncertainty was estimated following the JCGM 100:2008 standard guidelines (JCMG 100:2008 standard) and using as uncertainty estimator the standard deviation of the observed values with respect to the model prediction. The global model uncertainty was equal to 0.2 N.

Moreover, to evaluate the reliability of the run-out parameters (r_o and γ in Fig. 2a) predicted by the SWARM optimization, a comparison between experimental and analytical values is required. Since it is not possible to directly measure the value of run-out length and angle, the model outputs reliability was indirectly evaluated considering the width of the micro channels (Figure 5), which corresponds to two times the major tool radius (r_{CE1} in Fig. 3a). For this purpose, a comparison between the experimental value of r_{CE1}, derived from the measure of the channel width, and the model value of r_{CE1}, estimated applying Eq. 11 (see [16]) and using the r_o and γ values coming from the optimization toolbox, was made.

As reported in Table 3, very low percentage errors were obtained for each test (0.1%, 2.2%, and 5.5% respectively for Test A, Test B, and Test C), demonstrating that the model is robust and suitable for replicating and forecasting with high accuracy the actual cutting force components even if in presence of tool run-out phenomenon.

$$R_{CE1} = \left(\frac{d}{2} + r_0\right)\sqrt{1 + \left[\frac{d \cdot r_0 \cdot (cos\gamma - 1)}{\left(\frac{d}{2} + r_0\right)^2}\right]} \quad (11)$$

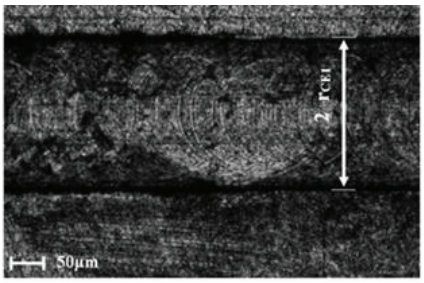

Fig. 5. Experimental measurement of major tool radius (r_{CE1}) from channel width.

Fig. 6 shows the comparison between experimental data and the optimized force model fitting curves for each test. The reported cutting force was obtained applying Eq.12.

$$F_C = \sqrt{{F_x}^2 + {F_y}^2} \quad (12)$$

The force component along z-axis was neglected because of its low value.

The experimental values of Fig. 6a show that during Test A the cutting forces are almost equally distribute on both cutting edges. Low run-out length and/or run out angle close to 90° determine this force distribution. The value of run-out parameters defined by PSO toolbox and reported in Table 2 confirm this hypothesis. In fact, a run-out length of 0.5 µm and a run-out angle of 74° were estimated as best values. Concerning the material parameters it is evident the high value of the specific cutting pressure with respect to the typical value that in meso/macro scale ranges from 1300 N/mm^2 to 1900 N/mm^2. This behavior can be explained considering the size effect resulting in higher values of specific cutting pressure in microscale than in meso/macro scales [2].

Table 3. Optimized parameters for Test "A", Test "B" and Test "C".

Parameter		Value		
		Test A	Test B	Test C
Material	Proportional Factor (p)	0.69	See Test A	
	Specific cutting pressure (K_{S0}) [N/mm^2]	4535	See Test A	
	Experimental coefficient (m)	4.93	See Test A	
Run-out	Run-out length (r_0) [µm]	0.52	1.58	2.27
	Run-out angle (γ)	73.9°	45.3°	0.1°
R_{CE1}	Model [µm]	95.1	96.3	97.4
	Measured [µm]	95.0	98.5	103.1
	Percentage error	0.1%	2.2%	5.5%

The most critical run-out effect was observed for Test C (Fig. 6c). This is also confirmed by the PSO toolbox outputs that for this test provided the highest value of run-out length (2.3 μm), almost completely on first cutting edge (run-out angle close to zero).

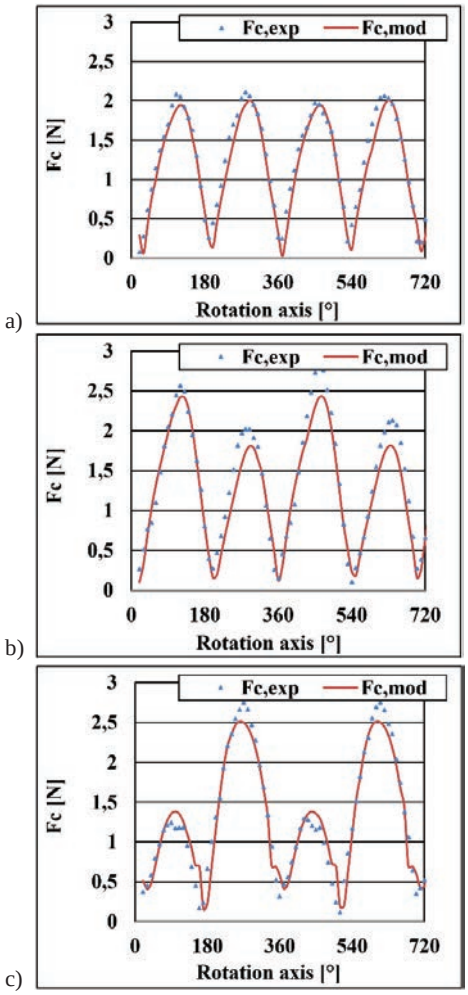

Fig. 6. Comparison between experimental data and force model; a) Test A; b) Test B; c) Test C.

4. Conclusions

This paper describes a procedure for optimizing by means of particle SWARM algorithm the parameter of an analytical model of cutting force in channels micro milling.

The cutting force model, based on the specific cutting pressure, takes in to account also the tool run-out contribution. For this purpose, the tool run-out influence on cutting edges trajectory and, as a consequence, on instantaneous chip thickness has been geometrically defined and modeled obtaining an analytical model of the cutting force components. The model parameters representing the tool-workpiece material interaction and the tool run-out effect have been optimized by means of data coming from experimental tests and using the particle SWARM optimization method.

The test with lower run-out effect was used to find the material parameters giving the best fitting between analytical and experimental data. Once defined the material parameters, the PSO toolbox of Matlab® was used in order to optimize the tool run-out parameters of each test made under the same cutting condition and characterized by different values of tool run-out.

The good agreement between the experimental data and the model demonstrates the reliability of the developed procedure in optimizing the force model parameters.

References

[1] Alting L, Kimura F, Hansen HN, Bissacco G. Micro Engineering. CIRP Annals 2003;52:635-657.
[2] Lai X, Li H, Li C, Lin Z, Ni J. Modelling and analysis of micro scale milling considering size effect, micro cutter edge radius and minimum chip thickness. Int J Mach Tool and Manu 2008;48(1):1-14.
[3] Komatsu T, Yoshino T, Matsumura T, Torizuka S. Effect of crystal grain size in stainless steel on cutting process in micromilling. CIRP Procedia (Fifth CIRP Conference on High Performance Cutting) 2012;1:150-155.
[4] Monroy K, Attanasio A, Ceretti E, Siller HR, Hendrichs N, GiardiniC. Evaluation of superficial and dimensional quality features in metallic micro-channels manufactured by micro-end-milling. Materials 2013;6(4):1434-1451.
[5] Garzòn M, Adams O, VeselovacD, Blattner M, Thiel R, Kirchheim A. High speed micro machining processes analysis for the precision manufacturing. CIRP Procedia (Fifth CIRP Conference on High Performance Cutting) 2012;1:609-614.
[6] Zhu K, Vogel-Heuser B. Sparse representation and its applications in micro-milling condition monitoring: noise separation and tool condition monitoring. Int J Adv Manu Tech 2014;70(1-4):185-199.
[7] Dhanorker A., Özel T. Meso/micro scale milling for micro-manufacturing. Int. J. Mech and Manu Systems 2008; 1(1):23-42.
[8] Park SS, Malekian M. Mechanistic modeling and accurate measurement of micro end milling forces. CIRP Annals 2009;58(1):49-52.
[9] Bao WY, Tansel IN. Modelling micro-end-milling operations. Part I: analytical cutting force model. Int J Mach Tools Manu 2000;40:2155-2173.
[10] Bao WY, Tansel IN. Modelling micro-end-milling operations. Part II: run-out. Int J Mach Tools Manu 2000;40:2175-2192.
[11] Bao WY, Tansel IN. Modelling micro-end-milling operations. Part III: influence of tool wear. Int J Mach Tools Manu 2000;40:2193-2211.
[12] Afazov SM, Ratchev SM, Segal J. Modelling and simulation of micro-milling cutting forces. J Mat Proc Tech 2010;210:2154-2162.
[13] Attanasio A, Gelfi M, Pola A, Ceretti E, Giardini C. Influence of material microstructures in micromilling of Ti6Al4V alloy. Materials 2013;6(4):4268-4283.
[14] Gelfi M, Attanasio A, Ceretti E, Garbellini A, Pola A. Micromilling of lamellar Ti6Al4V: cutting force analysis. Mat and Manuf Proc 2016;31(7):919-925.
[15] Kennedy L, Eberhart R. Swarm Intelligence. San Francisco: Morgan Kaufmann Publishers; 2001.
[16] Attanasio A, Garbellini A, Ceretti E, Giardini C. Force modelling in micromilling of channels. Int J Nanomanuf 2015; 11(5-6):275-296.